Optics Communications 528 (2023) 129010

Contents lists available at ScienceDirect

Optics Communications

journal homepage: www.elsevier.com/locate/optcom

Tunable optical nonlinearity and self-collimation of light in food dye solutions

Yujie Zhang [a], Guo Liang [b,d,*], Liqin Tang [a,*], Denghui Li [c], Jingyan Zhan [a], Daohong Song [a], Trevor Kelly [d], Huizhong Xu [d], Zhigang Chen [a,d,**]

[a] The MOE Key Laboratory of Weak-Light Nonlinear Photonics, TEDA Applied Physics Institute and School of Physics, Nankai University, Tianjin 300457, China
[b] School of Physics and Electrical Information, Shangqiu Normal University, Shangqiu 476000, China
[c] State Key Laboratory of NBC Protection for Civilian, Research Institute of Chemical Defense, Beijing 102205, China
[d] Department of Physics and Astronomy, San Francisco State University, San Francisco, CA 94132, USA

ARTICLE INFO

Keywords:
Optical nonlinearities
Self-collimating effects
Soft matter
Thermo-optic effect
Optical forces
Food dye

ABSTRACT

Food dyes are widely used in scientific research apart from the food colorant industry. In this work, we investigate nonlinear propagation of optical beams in food dye solutions of different colors, experimentally observing tunable nonlinearity and self-collimating effects of optical beams during propagation. We discuss possible mechanisms leading to optical nonlinearity by numerical simulation and theoretical analysis of the optical forces, and show that the nonlinearity in such solutions is mainly attributed to the thermo-optic effects. In addition, with appropriately mixed food dye solutions, we observe that nonlinear response arises at otherwise inactive wavelengths, leading to coupling of two self-collimated beams of different wavelengths. These results illustrate the possibility of employing low-cost food dye solutions for optical limiting and switching applications.

1. Introduction

The study of optical response of bio-soft matter, together with biological entities-based photonic probes and light guides, has attracted increasing attention in interdisciplinary fields of life sciences, chemistry and physics [1–7]. As with soft matter such as colloidal suspensions [8,9], various effects including Brownian motion, diffusion, optical forces and thermal effects typically play different roles in the complex media.

Two major competing effects have been concerned with respect to optical nonlinearity under laser illumination. One is the optical force-induced nonlinearity involving colloidal particles, and the other is the thermo-optic effect. A laser beam exerts optical forces (such as gradient and scattering forces [3]) on suspended particles, leading to artificial Kerr nonlinearity [10], which in turn have back reaction on the beam propagation dynamics [11–15]. Spatial variation in particle concentration can lead to a change of the local refractive index. For instance, with a positive polarizability of the suspended particles where their refractive index exceeds that of the background solution, the particles are attracted toward the high intensity regions. With a negative polarizability for which the particles have a refractive index lower than that of the background solution, they tend to be repelled from the beam path [11,13]. In both cases, the optical beam creates an increase of local refractive index at the region closer to the center of the beam, inducing a Kerr-like self-focusing nonlinearity. On the other hand, for the thermo-optic effect caused by temperature variation, the refractive index change takes the form of $n = n_0 + dn/dT \times \Delta T$ [16], where dn/dT is typically negative in most thermal solutions [17,18]. Thus, a self-defocusing nonlinearity often takes place because a nonuniform Gaussian-like optical beam results in a higher temperature along central high intensity regions of the beam path.

As a consequence of these two effects, a variety of nonlinear phenomena including optical spatial solitons [19] and shock waves [20] have been observed, in diverse nonlinear systems such as organic polymers [21], dielectric [11–14,22,23] and metallic [24–26] nanoparticle suspensions, and biological soft matter [1,2,4,27]. Certainly, the role of these two effects varies in different systems. For instance, the gradient force gives rise to stable soliton formation in a negative polarizability suspension in which polytetrafluoroethylene (PTFE) particles are suspended in a glycerin–water solution, almost without the influence of thermal effects [13]. Nevertheless, in some plasmonic media, such as gold nanosuspensions illuminated by light of certain wavelengths, both effects should be taken into account because of the enhanced optical forces and the extensive heat generated from plasmonic resonant absorption [24,26,28–30].

* Corresponding authors.
** Corresponding author at: The MOE Key Laboratory of Weak-Light Nonlinear Photonics, TEDA Applied Physics Institute and School of Physics, Nankai University, Tianjin 300457, China.
E-mail addresses: liangguo0916@163.com (G. Liang), tanya@nankai.edu.cn (L. Tang), zgchen@nankai.edu.cn (Z. Chen).

https://doi.org/10.1016/j.optcom.2022.129010
Received 15 June 2022; Received in revised form 13 September 2022; Accepted 15 September 2022
Available online 24 September 2022

Another kind of nonlinear optical material is the so-called NLOphores, which are mainly inorganic, organic, and organometallic compounds dyes. Their designable structures and variable synthetic compounds can bring diverse and tunable optical properties and applications [31,32]. For instance, they are widely applied in biomedical research thanks to their suitable florescent and specific targeting ability [33]. In addition, Phthalocyanines, as robust macrocyclic dyes have also been explored for nonlinear optical applications [34]. On the other hand, dyes applied in food coloring (food dye) are nontoxic, low-cost, and commercially available, yet their nonlinear optical properties in aqueous solutions are rarely investigated.

In this work, we study nonlinear beam dynamics in food dye solutions, revealing a tunable optical nonlinearity and formation of a self-collimated beam (SCB) in such solutions with low-power continuous-wave (CW) laser illumination. By conducting a series of experiments with food dye solutions of different colors (pigments), we demonstrate that the optical nonlinearities of food dye solutions are mainly attributed to the thermo-optic effects, dependent on the pigment, the concentration, and the wavelength of the laser illumination. In addition, with appropriately mixed food dye solutions, we observe that a nonlinear response arises for otherwise inactive wavelengths, leading to nonlinear coupling between two self-collimated beams of different wavelengths. Using numerical simulation and calculation, we show that the nonlinear self-collimating effect is mainly attributed to the shifting of the focal point induced by the absorption-dependent thermo-optic effect [35], while the optical forces on the food dye particles seem to have negligible contribution to the optical nonlinearity.

2. Experimental setup and results

2.1. Color-dependent absorption of food dye solutions

Food dyes with four different colors (red, yellow, green, and blue, McCormick, made in the USA) are purchased from a nearby convenience store. In our experiments, the liquid food dyes are directly diluted into deionized water to prepare the samples with different concentrations. The absorption spectra of the four samples prepared with a concentration of 3×10^{-4} g/mL are measured by a spectrometer as summarized in Fig. 1. Different food dye samples exhibit distinct absorption spectra with peak absorptions at different wavelengths and varying absorbance levels at three laser wavelengths of 488 nm, 532 nm, and 639 nm used in our subsequent measurements. At $\lambda = 532$ nm, the red dye is the most absorptive, the blue takes second place, while the green and yellow have weak absorption. For the other wavelengths of 488 nm and 639 nm, the absorption strengths take different orders for the four dyes.

2.2. Nonlinear beam propagation in different food dye solutions

Firstly, we examine the beam propagation dynamics through food dye solutions (concentration is 7×10^{-4} g/mL) at different input powers. The setup is illustrated in Fig. 2(a). A Gaussian beam (laser 1) operating at $\lambda = 639$, 532, or 488 nm is collimated by a pair of lenses (L_1, L_2), then focused into a 3-cm-long glass cuvette filled with the food dye solutions by a convex lens L_5. An optical attenuator is used to tune the optical power. The focal point of the input beam is located about 1 cm away from the input facet inside the cuvette. The output beam after propagating through the sample is collected by a lens L_6, and recorded by a CCD camera.

We take two kinds of dye solutions, red and yellow, which have strong absorption and nearly no absorption at 532 nm, respectively. Beam propagation exhibits notably different behaviors as shown in Figs. 2(b)–2(e). In the red dye solution, the input beam (with a diameter about 0.35 mm) [Fig. 2(b)] diffracts strikingly at low power (~0.01 mW) [Figs. 2(c1) and 2(f)]. As the input power increases, local refractive index changes and the output beam size shrinks dramatically,

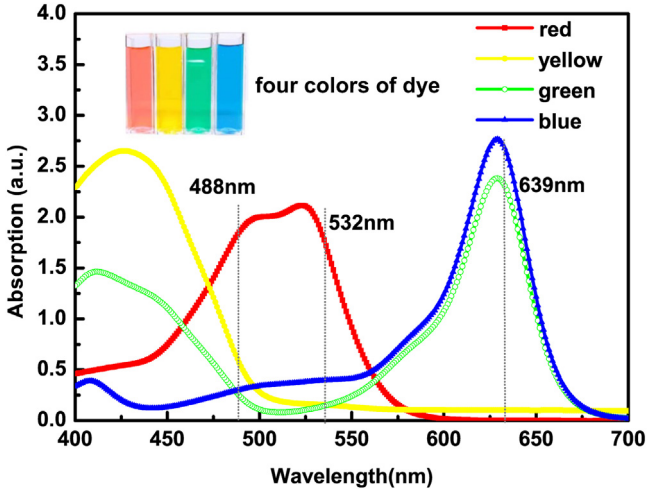

Fig. 1. Absorption spectra for dye solutions of four different colors at the same concentration of 3×10^{-4} g/mL. The vertical dashed lines indicate absorbance at the laser wavelengths of 488, 532, and 639 nm available for experiments. The inset shows a picture of the four food dye solutions used in experiments.

reaching a minimum at 100 mW [Fig. 2(c2)]. Subsequently, when the power is further increased, the beam starts to diverge, and gradually evolves into an expanded asymmetrical diffraction ring pattern due to thermal defocusing nonlinearity accompanied by fluid convection [Fig. 2(c3)]. Such asymmetric patterns were observed and discussed in several prior experiments [2,36,37], so it will not be the focus of this work. In contrast, a totally different outcome is observed in the yellow dye solution at the same concentration and with the same wavelength. The output beam remains almost unchanged when the input power is increased, as shown in the third row [Figs. 2(e1)–2(e3)]. It implies that there is no evident optical nonlinearity that exists in the yellow dye solution due to weak absorption at this wavelength. These results indicate clearly that the observed optical nonlinearity is related to absorption.

Next, we perform systematic experiments with all four colors of food dye solutions using 639 nm and 488 nm lasers to compare the beam dynamics. The measured output beam diameters (full width at $1/e^2$-intensity) as a function of input powers in these solutions are summarized in Figs. 3(a)–(c). Fig. 3(a) shows that the focusing nonlinearity strength at $\lambda = 532$ nm (examined from the smallest beam size) decreases in the following order of red, blue, green, and yellow dyes. At $\lambda = 488$ nm, as shown in Fig. 3(b), the focusing nonlinearity strength decreases in the order of red, yellow, blue, and green. While at $\lambda = 639$ nm, Fig. 3(c) shows that the nonlinearity strength decreases in the order of blue, green, yellow, and red dyes. Comparison of the nonlinearity strength with the absorption spectrum in Fig. 1 reveals that these two are positively correlated. In other words, a stronger absorption leads to a stronger optical nonlinearity, allowing us to vary the pump laser to tune the optical nonlinearity. Furthermore, to investigate the effect of dye concentrations on their generated nonlinearity strength, we also measure output beam diameters as a function of the input laser power at different concentrations. Typical results are shown in Fig. 3(d) for the blue dye solutions. As indicated by the change of output beam diameters, we see that the optical nonlinearity depends strongly on dye concentration, therefore we can also tune the optical nonlinearity by varying concentrations.

Now, we discuss the apparent self-focusing dynamics observed in above experiments, i.e., an optical beam undergoes a converging effect before it expands at sufficiently high input power. In fact, this originates from the shifting of the focal point induced by the thermo-optic effect. The refractive index in the center of the medium is lower than that far from the center at high input power, so the originally focused

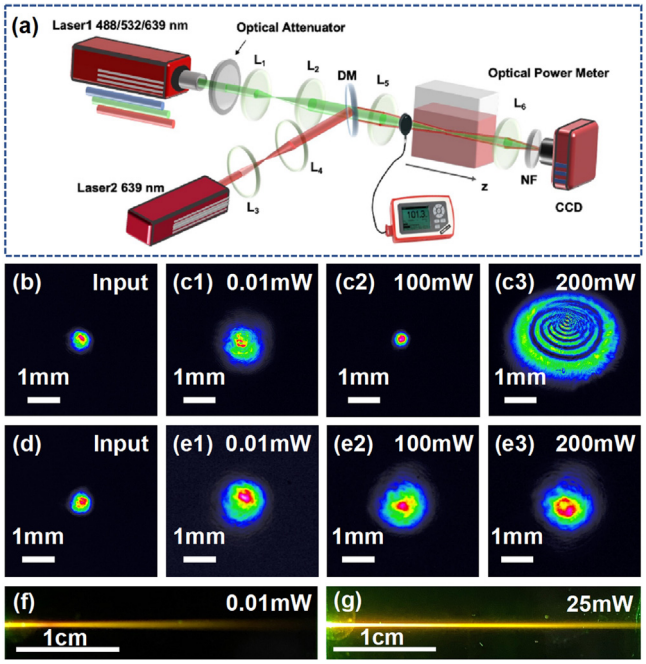

Fig. 2. (a) Schematic of the experimental setup. (L_1, L_2) and (L_3, L_4) are two pairs of collimating lenses. L_5: focusing lenses; L_6: imaging lens; The lenses are all double-glued achromatic lenses to eliminate achromatic aberration of different wavelengths. DM: dichroic mirror; NF: notch filter; CCD: charge-coupled device. Laser 1 is used as the main beam for nonlinear propagation experiment, and Laser 2 is employed when needed for two beam coupling experiment. (b)–(e) Nonlinear propagation results at different optical powers, where (b) and (d) are inputs, and (c1)–(c3) and (e1)–(e3) are output intensity patterns of a laser beam at 532 nm, through red and yellow dye solutions, respectively. (f)–(g) Side-view images taken at 0.01 mW and 25 mW for the red dye solution.

beam undergoes self-defocusing. The strong negative nonlinearity near the focal point pushes the beam converging forward, just like what a concave lens located before the focus of a beam does [35], thus reducing the apparent beam size at output [Fig. 2(c3)]. Interestingly, when optical power is increased to 25 mW, focusing induced by the convergent lens and self-defocusing induced by the thermal lens balance, so the output pattern becomes almost as same as the input, and the initially converging beam becomes collimated over a distance, in a soliton-like profile, which is called self-collimation [Fig. 2(g)] [30,35]. Such a self-collimated beam can penetrate deeply into the solution, maintaining its beam pattern with very little distortion. This thermo-optic effect is further confirmed by experiments where the original focal point is located before the input facet. In such experiments, we find the SCB cannot be formed. Instead, the beam will undergo defocusing during its entire propagation through the solution.

2.3. Nonlinear coupling of two beams of different wavelengths in mixed dye solutions

Since the nonlinearity of food dye solutions is directly related to their absorption, it should be tunable by mixing different dye solutions. In principle, a strong nonlinearity of dye solutions can be achieved at the wavelengths of interest in such synthetic food dye solutions with appropriate proportions. Here, we illustrate a simple example by mixing red and green food dyes with equal proportions as shown in Fig. 4(a). The spectra of the mixture and each individual solution are also measured and shown in Fig. 4(b). The two beams propagate collinearly in the mixed solution and they experience a refractive-index modulation created by both beams. One of pairing beams is at 532 nm (beam 1), and the other is at 639 nm (beam 2) [Fig. 2(a)]. At a low input power, both beams diffract linearly while propagating through the mixed solution, as shown in the second column in Fig. 4(c). When the two beams are decoupled, that is, any one of the two beams is blocked, the remaining beam only displays partial nonlinearity [third column in Fig. 4(c)]. However, when the two beams are coupled, the optical beams exhibit stronger nonlinearity [fourth column in Fig. 4(c)]. These results resemble the incoherently coupled spatial soliton pairs observed early in a biased photorefractive crystal [38], but here it is due to the enhanced shifting of the focal point toward the output plane as a result of combined thermo-optic effects from both beams. Especially, in our experiments, when the input power is increased to 23.7 mW for beam 1 and 55.4 mW for beam 2, two self-collimated beams of different wavelengths seem to be coupled to each other, exhibiting the coupled soliton-pair-like behavior. It appears that the beam profile in Fig. 4(c4) is smaller than that in Fig. 4(c3). This may be due to the following two reasons: firstly, Beam1 at 532 nm is focused to a smaller size at the input; secondly, from Fig. 4(b), we can see that the absorption at 639 nm is much larger than that at 532 nm, so even the power is less than 1 mW for test of linear propagation, thermal effects may have worked slightly on beam 2 at this longer wavelength.

2.4. Z-scan measurement of the nonlinear coefficient

To determine the nonlinear coefficient, we perform closed z-scan measurements of dye solutions, whose movements are restricted in a 1-mm-thick cuvette [Fig. 5(a)]. The normalized power transmittance is determined by [39,40]

$$T(z) = \frac{\int_0^{r_a} |E_a(\Delta\phi_0, r, z)|^2 r dr}{S\int_0^{\infty} |E_a(0, r, z)|^2 r dr} \tag{1}$$

where E_a is the optical field at the aperture, r_a is the aperture radius, $\Delta\phi_0$ is the on-axis phase shift at the focus and S is the aperture transmittance in the linear regime. The measured power transmittance, as shown in Fig. 5(b), exhibits a peak-to-valley structure, implying the self-defocusing nonlinearity of the solutions [41,42]. It is noted that the asymmetric curve of red dye is due to the absorption saturation under 532 nm. But at this wavelength, other colors have little absorption so the asymmetry is not obvious. Food dyes with stronger absorption will exhibit stronger nonlinearity, so under 532 nm laser, the red dye shows the supreme optical nonlinearity. Representatively, the nonlinear refraction coefficient of red dye solution is $n_2 = -2.14 \times 10^{-7}$ cm ^{2}/W for the input power of 100 mW calculated by Eq. (1).

3. Simulation and numerical results

We take the red dye solution for example to illustrate the thermal nonlinearity and the formation of SCB in simulation. The medium absorbs energy and undergoes a non-radiative transition simultaneously with heat generation and the subsequent formation of a thermal gradient under an inhomogeneous light field. With a Gaussian profile, the center of the beam has a higher intensity, resulting in a higher temperature and a lower refractive index, and if we assume the media suits Kerr-like nonlinearity, $n = n_0 + dn/dT \times \Delta T$ can be adapted to [37,43]

$$n = n_0 + n_2 I \tag{2}$$

where n_0 is the linear refractive index, n_2 is the nonlinear refraction coefficient which is almost negative in thermal media and I is the local intensity.

In an absorption media with such an optical nonlinearity, the paraxial propagation equation along z is [11]

$$i\frac{\partial}{\partial z}\psi + \frac{1}{2k}\nabla_{\perp}^2\psi + k\frac{\Delta n}{n_0}\psi + i\frac{\alpha_0}{2}\psi = 0 \tag{3}$$

where ψ is the amplitude of the wave, α_0 is the linear absorption coefficient, k is the wavenumber, $\Delta n = n_2 I$. We numerically simulate the beam propagation behavior in red dye solutions using the Beam

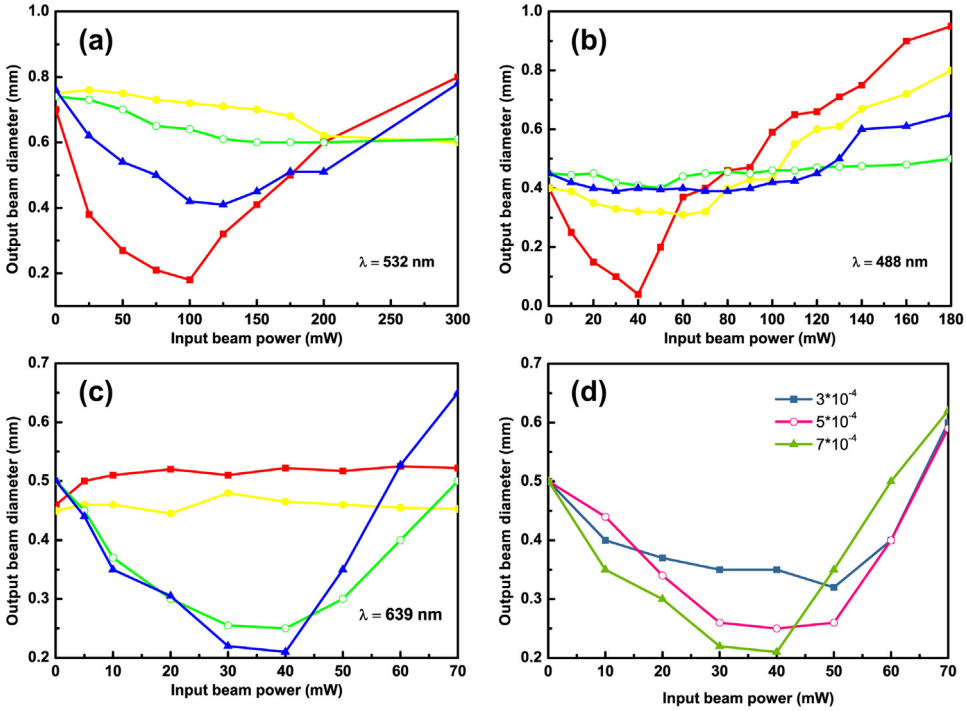

Fig. 3. Measured output beam diameter as a function of the input laser power for dye solutions of four different colors at the same concentration for three laser wavelengths of (a) 532 nm, (b) 488 nm, and (c) 639 nm. (d) The output beam diameter as a function of the input laser power at $\lambda = 639$ nm in blue dye solutions of different concentrations: 3×10^{-4} g/mL, 5×10^{-4} g/mL, 7×10^{-4} g/mL.

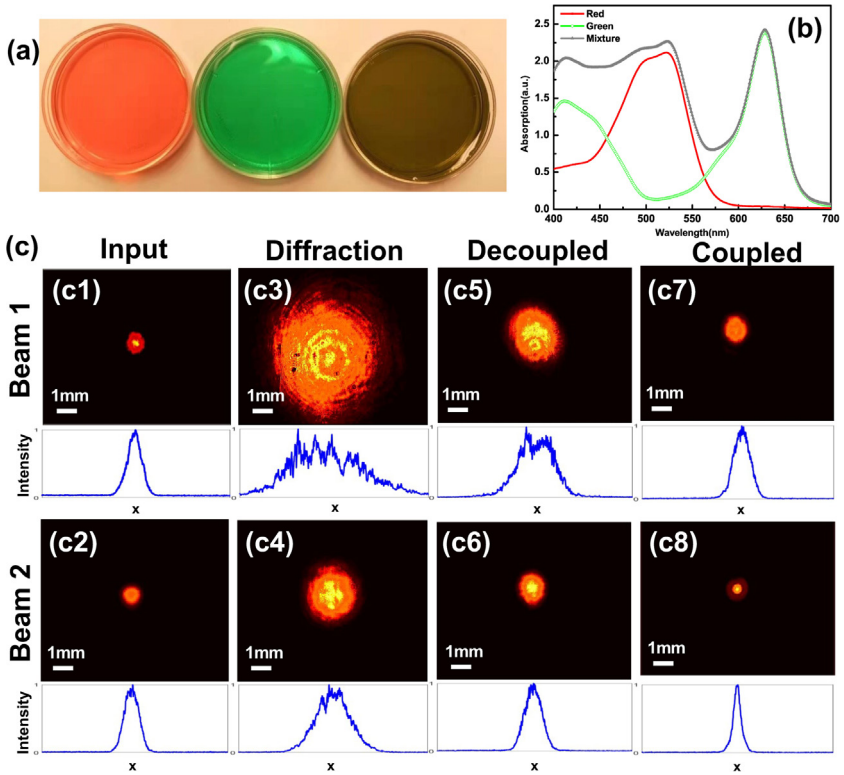

Fig. 4. (a) Red, green food dye solutions and their mixture with equal proportions. (b) Absorption spectra of red dye, green dye, and their mixed solution. (c) Nonlinear coupling of two laser beams of wavelengths 532 nm (beam 1) and 639 nm (beam 2) in a mixture of red and green food dye solutions. Shown in (c) from left to right are transverse intensity patterns and corresponding beam profiles taken for input, normal diffraction, decoupled output (when the other pairing beam is blocked), and the coupled soliton-pair-like behavior (when both beams are in action). The "x" is the abscissa of the profile image.

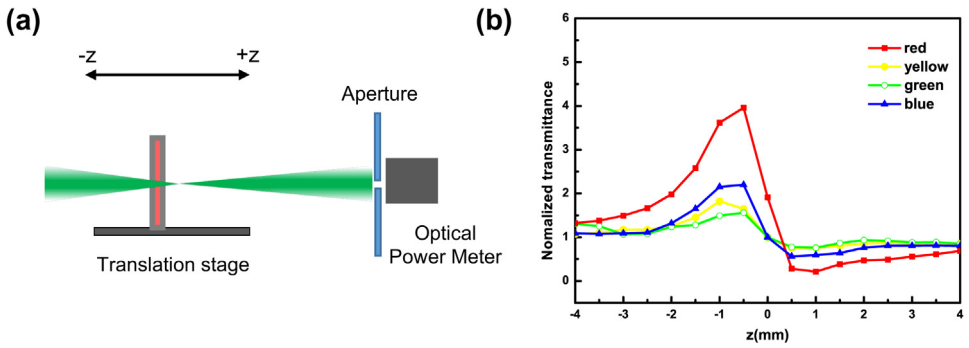

Fig. 5. (a) Illustration of the Z-scan setup. (b) Measured Z-scan results of a 1-mm-thick cell filled with food dye solutions of four different colors at 532 nm, all displaying a negative nonlinear coefficient.

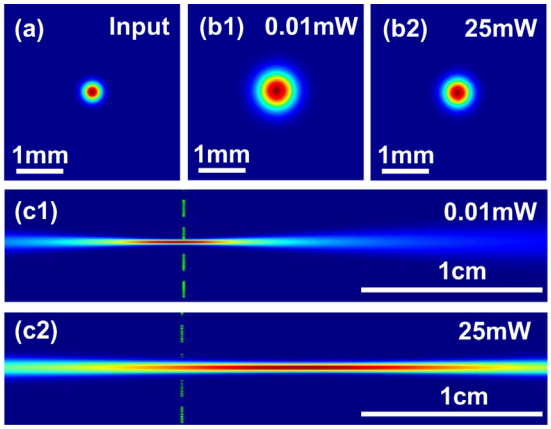

Fig. 6. Simulated behavior of a 532 nm laser beam propagating through a red dye solution. (a) Input transverse intensity pattern. (b1)-(b2) Corresponding output beam patterns at different optical powers. (c1)-(c2) The corresponding side view of the beam propagating through a 3-cm-long cuvette. The green dashed lines in (c1) and (c2) mark the position of original focus of the beam in the linear case.

Propagation Method [44]. The critical parameters during simulation include $n_0 = 1.33$ for linear refractive index, $n_2 = -2.14 \times 10^{-7}$ cm^2/W measured by the closed z-scan experiment, and $\alpha_0 = 2$ cm^{-1}. A Gaussian beam focused by a lens (focal length is 12 cm), diffracts 11 cm linearly in free space, and then transmits in the food dye solutions for 3 cm with a loss in every step. The simulation results are represented in Figs. 6(a)–6(c). The input beam diameter is 0.35 mm [see Fig. 6(a)], and diverges into 0.7 mm in linear diffraction at low input power [Fig. 6(b1)]. When we increase the optical power of the input beam, the intensity near the focal point is extremely enhanced, so giant nonlinearity pushes the focal point forward. After propagating a long distance, the beam will be less divergent compared with the linear case, which is in consistence with experimental results. When the input power is increased to 25 mW, diffraction and focusing reach a balance. One can see that the output beam diameter is almost the same as the input one and a self-collimated beam is formed [see Fig. 6(b2)]. From the side view of the beam at input powers of 0.01 mW [Fig. 6(c1)] and 25 mW [Fig. 6(c2)], it is clear that the intensity is more converging in smaller area as a result of SCB formation in the red dye solution, which is in good agreement with experimental results in Figs. 2(f)–2(g).

4. Discussion

As mentioned above, in order to make clear the beam propagation behavior in food dye solutions, we need to determine whether optical force also plays an important role for nonlinear beam dynamics in food dye solutions. Actually, in dielectric nanosuspensions under CW laser illumination, optical forces, including gradient and scattering forces may create a spatial variation in particle concentration, leading to local changes of refractive index, as explained earlier. Here, we only discuss the gradient and absorption forces since for food dye solutions, the scattering force is negligible [45], which is different from plasmonic and biological suspensions [1,2]. The particle's size in food dye solutions is only several nanometers, which is much smaller than the pump laser's wavelength. In the Rayleigh regime, the gradient force is given as $\boldsymbol{F}_{grad} = (\alpha/4)\nabla|\boldsymbol{E}^2|$, where $|\boldsymbol{E}^2|$ corresponds to the optical intensity, α is effective polarizability of the particle and is given as $\alpha = 4\pi\varepsilon_0 n_b^2(m^2\text{-}1)/(m^2\text{+}2)R^3$, and $m = n_p/n_b$ [13]. The refractive indexes of the particle and the background medium are $n_p = 1.56$ [46] and $n_b = 1.33$, respectively, and $R = 5$ nm is the particle radius in our numerical calculation. It should be pointed that, we measured the average particle through dynamic light scattering (DLS) method by Malvern Mastersizer but found no signals, indicating that detectable dye particles if any were smaller than 5 nm, so here, we use $R = 5$ nm as the estimation of maximum particle size for calculation. The maximum gradient force is estimated to be about 10^{-9} pN at the location of the focal point. Under the action of this force, the maximum speed of the particle will be only $\sim 10^{-11}$ m/s from Stokes' law [30] ($\boldsymbol{F}_{grad} = 6\pi\mu R v$, where $\mu = 1.005 \times 10^{-3}$ Pa s is viscosity of water, and v is the velocity of the particle).

As for absorption force, $\boldsymbol{F}_{abs} = \hat{z}(n_b/c)C_{abs}I$ [47], is along the propagation direction, where C_{abs} is the absorption cross-section and can be obtained from absorption spectra [47], and I is the optical intensity. For food dyes in our experiments, we find that when optical power is 100 mW, the maximum $\boldsymbol{F}_{abs} \sim 10^{-10}$ pN, which is 10 times smaller than the gradient force. Obviously, these two forces are too small to pull or push the particles, so the local change of refractive index induced by optical force is impossible, or rather, it can be neglected compared to that created by the thermo-optic effect. As such, we believe the observed nonlinear self-collimating effect is mainly attributed to the shifting of the focal point induced by the absorption-dependent thermo-optic effect, in accordance with early work based on colloidal suspensions of gold nanoparticles [35].

We also point out that here the discussion about optical forces is motivated by any "nonlinear refractive-index changes" due to the movement and density changes of possible suspended particles induced by optical forces [1–4,11,13,24]. This is quite different from the "nonlinear optical force" calculated for trapped nanoparticles under the action of femtosecond pulses [48].

5. Conclusion

We have explored tunable optical nonlinearity exhibited when an optical beam propagates through food dye solutions of different colors. Our results show the optical nonlinearity is attributed to the thermo-optic effect, which causes the focal point to shift forward, leading to apparent self-collimation of light beams in such solutions. Furthermore,

we observe soliton-pair-like interaction between two self-collimated beams of different wavelengths, due to the enhanced shifting of the focal point toward the output plane of the paired beams. By calculating the gradient force and absorption force, we find that the optical forces do not seem to play a dominant role in leading to the local change of refractive index as previously thought, which is in contrast with previously reported work on optical force-induced nonlinearity and self-trapping of optical beams in dielectric and plasmonic suspensions. This readily available and tunable optical nonlinearity in low-cost food dye solutions can be potentially used in a wide range of applications such as optical limiting and switching.

Funding

This work was supported by the National Key R&D Program of China (2017YFA0303800); the National Natural Science Foundation of China (12134006 and 11922408); Natural Science Foundation of Tianjin (21JCYBJC00060); Key Research Fund of Higher Education of Henan Province, China (23A140021); Open Subject of the Key Laboratory of Weak Light Nonlinear Photonics of Nankai University (OS 21-3).

Declaration of competing interest

The authors declare that they have no known competing financial interests or personal relationships that could have appeared to influence the work reported in this paper.

Data availability

No data was used for the research described in the article.

References

[1] A. Bezryadina, T. Hansson, R. Gautam, B. Wetzel, G. Siggins, A. Kalmbach, J. Lamstein, D. Gallardo, E.J. Carpenter, A. Ichimura, R. Morandotti, Z. Chen, Nonlinear self-action of light through biological suspensions, Phys. Rev. Lett. 119 (5) (2017) 058101.
[2] R. Gautam, Y. Xiang, J. Lamstein, Y. Liang, A. Bezryadina1, G. Liang, T. Hansson, B. Wetzel, D. Preece, A. White, M. Silverman, S. Kazarian, J. Xu, R. Morandotti, Z. Chen, Optical force-induced nonlinearity and self-guiding of light in human red blood cell suspensions, Light Sci. Appl. 8 (1) (2019) 1–9.
[3] H. Xin, Y. Li, Y. Liu, Y. Zhang, Y. Xiao, B. Li, Optical forces: From fundamental to biological applications, Adv. Mater. 32 (37) (2020) 2001994.
[4] R. Gautam, A. Bezryadina, Y. Xiang, T. Hansson, Y. Liang, G. Liang, J. Lamstein, N. Perez, B. Wetzel, R. Morandotti, Z. Chen, Nonlinear optical response and self-trapping of light in biological suspensions, Adv. Phys. X 5 (1) (2020) 1778526.
[5] P. Zemánek, G. Volpe, A. Jonáš, O. Brzobohatý, Perspective on light-induced transport of particles: from optical forces to phoretic motion, Adv. Opt. Photon. 11 (3) (2019) 577–678.
[6] T. Pan, D. Lu, H. Xin, B. Li, Biophotonic probes for bio-detection and imaging, Light Sci. Appl. 10 (1) (2021) 1–22.
[7] C.F. Guimarães, R. Ahmed, A.P. Marques, R.L. Reis, U. Demirci, Engineering hydrogel-based biomedical photonics: Design, fabrication, and applications, Adv. Mater. 33 (23) (2021) 2006582.
[8] C. Conti, R. Giancarlo, S. Trillo, Optical spatial solitons in soft matter, Phys. Rev. Lett. 95 (18) (2005) 183902.
[9] C. Conti, E. DelRe, Optical supercavitation in soft matter, Phys. Rev. Lett. 105 (11) (2010) 118301.
[10] P.W. Smith, P.J. Maloney, A. Ashkin, Use of a liquid suspension of dielectric spheres as an artificial Kerr medium, Opt. Lett. 7 (8) (1982) 347–349.
[11] R. El-Ganainy, D.N. Christodoulides, C. Rotschild, M. Segev, Soliton dynamics and self-induced transparency in nonlinear nanosuspensions, Opt. Express 15 (16) (2007) 10207–10218.
[12] M. Matuszewski, W. Krolikowski, Y.S. Kivshar, Spatial solitons and light-induced instabilities in colloidal media, Opt. Express 16 (2) (2008) 1371–1376.
[13] W. Man, S. Fardad, Z. Zhang, J. Prakash, M. Lau, P. Zhang, M. Heinrich, D.N. Christodoulides, Z. Chen, Optical nonlinearities and enhanced light transmission in soft-matter systems with tunable polarizabilities, Phys. Rev. Lett. 111 (21) (2013) 218302.
[14] E. Greenfield, J. Nemirovsky, R. El-Ganainy, D.N. Christodoulides, M. Segev, Shockwave based nonlinear optical manipulation in densely scattering opaque suspensions, Opt. Express 21 (20) (2013) 23785–23802.
[15] Y. Lamhot, A. Barak, O. Peleg, M. Segev, Self-trapping of optical beams through thermophoresis, Phys. Rev. Lett. 105 (16) (2010) 163906.
[16] S.J. Sheldon, L.V. Knight, J.M. Thorne, Laser-induced thermal lens effect: a new theoretical model, Appl. Opt. 21 (9) (1982) 1663–1669.
[17] N. Ghofraniha, C. Conti, G. Ruocco, F. Zamponi, Time-dependent nonlinear optical susceptibility of an out-of-equilibrium soft material, Phys. Rev. Lett. 102 (3) (2009) 038303.
[18] Y.H. Kim, S.J. Park, S.W. Jeon, S. Ju, C.S. Park, W.T. Han, B.H. Lee, Thermo-optic coefficient measurement of liquids based on simultaneous temperature and refractive index sensing capability of a two-mode fiber interferometric probe, Opt. Express 20 (21) (2012) 23744–23754.
[19] Z. Chen, M. Segev, D.N. Christodoulides, Optical spatial solitons: historical overview and recent advances, Rep. Progr. Phys. 75 (8) (2012) 086401.
[20] G. Marcucci, D. Pierangeli, S. Gentilini, N. Ghofraniha, Z. Chen, C. Conti, Optical spatial shock waves in nonlocal nonlinear media, Adv. Phys. X 4 (1) (2019) 1662733.
[21] V. Smith, B. Leung, P. Cala, Z. Chen, W. Man, Giant tunable self-defocusing nonlinearity and dark soliton attraction observed in m-cresol/nylon thermal solutions, Opt. Mater. Express 4 (9) (2014) 1807–1812.
[22] P.J. Reece, E.M. Wright, K. Dholakia, Experimental observation of modulation instability optical spatial soliton arrays in soft condensed matter, Phys. Rev. Lett. 98 (20) (2007) 203902.
[23] A.S. Reyna, C.B. De Araújo, Guiding and confinement of light induced by optical vortex solitons in a cubic–quintic medium, Opt. Lett. 41 (1) (2016) 191–194.
[24] S. Fardad, A. Salandrino, M. Heinrich, P. Zhang, Z. Chen, D.N. Christodoulides, Plasmonic resonant solitons in metallic nanosuspensions, Nano Lett. 14 (5) (2014) 2498–2504.
[25] T.S. Kelly, Y.X. Ren, A. Samadi, A. Bezryadina, D. Christodoulides, Z. Chen, Guiding and nonlinear coupling of light in plasmonic nanosuspensions, Opt. Lett. 41 (16) (2016) 3817–3820.
[26] H. Xu, P. Alvaro, Y. Xiang, T.S. Kelly, Y. Ren, C. Zhang, Z. Chen, Plasmonic resonant nonlinearity and synthetic optical properties in gold nanorod suspensions, Photon. Res. 7 (1) (2019) 28–35.
[27] N. Perez, J. Chambers, Z. Chen, A. Bezryadina, Nonlinear self-trapping and guiding of light at different wavelengths with sheep blood, Opt. Lett. 46 (3) (2021) 629–632.
[28] T. Jia, T. He, P. Li, Y. Mo, Y. Cui, A study of the thermal-induced nonlinearity of Au and Ag colloids prepared by the chemical reaction method, Opt. Laser Technol. 40 (7) (2008) 936–940.
[29] L. Agiotis, M. Meunier, Nonlinear thermal lensing of high repetition rate ultrafast laser light in plasmonic nano-colloids, Nanophotonics 11 (5) (2022) 1051–1062.
[30] V. Shvedov, K. Cyprych, M. Yadira Salazar-Romero, Y. Izdebskaya, W. Krolikowski, Nonlinear propagation and quasi self-confinement of light in plasmonic resonant media, Opt. Express 26 (18) (2018) 23196–23206.
[31] C.W. Ghanavatkar, V.R. Mishra, N. Sekar, Review of NLOphoric azo dyes–developments in hyperpolarizabilities in last two decades, Dyes Pigm. 191 (2021) 109367.
[32] U. Warde, N. Sekar, NLOphoric mono-azo dyes with negative solvatochromism and in-built ESIPT unit from ethyl 1, 3-dihydroxy-2-naphthoate: Estimation of excited state dipole moment and pH study, Dyes Pigm. 137 (2017) 384.
[33] F.F. Sperandio, Y.Y. Huang, M.R. Hamblin, Antimicrobial photodynamic therapy to kill gram-negative bacteria, Recent Pat. Antiinfect. Drug Discov. 8 (2) (2013) 108–120.
[34] M. Yahya, Y. Nural, Z. Seferoğlu, Recent advances in the nonlinear optical (NLO) properties of phthalocyanines: A review, Dyes Pigm. 198 (2022) 109960.
[35] A.B. Ortega, E.C. Brambila, V.L. Gayou, R.D. Macuil, A.O. Diaz, A.Z. Alvarez, A.V. Arzola, K. Volke-Sepúlveda, Light control through a nonlinear lensing effect in a colloid of biosynthesized gold nanoparticles, J. Mod. Opt. 66 (5) (2019) 502–511.
[36] G. Wang, S. Zhang, F.A. Umran, X. Cheng, N. Dong, D. Coghlan, Y. Cheng, L. Zhang, W.J. Blau, J. Wang, Tunable effective nonlinear refractive index of graphene dispersions during the distortion of spatial self-phase modulation, Appl. Phys. Lett. 104 (14) (2014) 141909.
[37] R. Karimzadeh, Spatial self-phase modulation of a laser beam propagating through liquids with self-induced natural convection flow, J. Opt. 14 (9) (2012) 095701.
[38] Z. Chen, M. Segev, T.H. Coskun, D.N. Christodoulides, Observation of incoherently coupled photorefractive spatial soliton pairs, Opt. Lett. 21 (18) (1996) 1436–1438.
[39] M. Sheik-Bahae, A.A. Said, E.W. Van Stryland, High sensitivity, single beam n2 measurements, Opt. Lett. 14 (17) (1989) 955–957.
[40] J. Yang, Y. Song, Direct observation of the transient thermal-lensing effect using the phase-object Z-scan technique, Opt. Lett. 34 (2) (2009) 157–159.
[41] H.A. Badran, Z-scan measurement for the thermo-optic coefficient and transmitted beam profile of 1.8-dihydroxy-naphthalin-3, 6 disulfonic acid-[2-(4-azo)]-N-(5-methyl-3-isoxazolyl)-benzene sulfonamide, Adv. Phys. Theor. Appl. 26 (2013) 36–44.
[42] C.W. Ghanavatkar, V.R. Mishra, S. Sharma, E. Mathew, S. Chitrambalam, I.H. Joe, S.N. Nethi, Red emitting hydroxybenzazole (HBX) based azo dyes: Linear and NonLinear optical properties, optical limiting, Z scan analysis with DFT assessments, J. Fluoresc. 30 (2) (2020) 335–346.

[43] L. Sarkhosh, H. Aleali, R. Karimzadeh, N. Mansour, Large thermally induced nonlinear refraction of gold nanoparticles stabilized by cyclohexanone, Phys. Stat. Sol. (A) 207 (10) (2010) 2303–2310.
[44] T.C. Poon, Engineering optics with MATLAB, World Scientific, 2006.
[45] E.C. Le Ru, P.G. Etchegoin, Raman Spectroscopy and Related Optical Techniques, Elsevier, 2009.
[46] A. Djorović, M. Meyer, B.L. Darby, E.C. Le Ru, Accurate modeling of the polarizability of dyes for electromagnetic calculations, ACS Omega 2 (5) (2017) 1804–1811.
[47] Y. Harada, T. Asakura, Radiation forces on a dielectric sphere in the Rayleigh scattering regime, Opt. Commun. 124 (5–6) (1996) 529–541.
[48] A. Devi, A.K. De, Unified treatment of nonlinear optical force in laser trapping of dielectric particles of varying sizes, Phys. Rev. Res. 3 (3) (2021) 033074.